

# Investigation of the adsorption behaviour of a chiral model compound on a tartardiamide-based network-polymeric chiral stationary phase

Johan Lindholm, Torgny Fornstedt\*

*Department of Surface Biotechnology, Uppsala University, BMC, Box 577, SE-751 23 Uppsala, Sweden*

Received 8 April 2005; received in revised form 25 July 2005; accepted 28 July 2005

Available online 16 September 2005

## Abstract

The adsorption behaviour of the enantiomers of 2-phenylbutyric acid on the chiral stationary phase (CSP) Kromasil CHI-TBB was studied using hexane/MTBE (90/10) as eluent. Adsorption isotherms were acquired at 40 different enantiomer concentrations in the interval between 7.6  $\mu$ M and 305 mM, an approximately 40,000-fold dynamic range. The adsorption data fitted well to the bi-Langmuir model, indicating a heterogeneous surface with two different types of adsorption sites having different equilibrium constants and capacities; namely one chiral site and one non-chiral site. A comparison with earlier adsorption studies on modern CSPs revealed that the capacity value of the “true” chiral site of Kromasil CHI-TBB is the largest reported so far. The elution profiles simulated with these parameters show excellent agreement with the corresponding experimental profiles. Guidelines for comparisons of loading capacities of CSPs are presented.

© 2005 Elsevier B.V. All rights reserved.

**Keywords:** Chiral LC; Kromasil CHI-TBB; 2-Phenylbutyric acid; Nonlinear theory; Adsorption isotherms; Chiral capacity

## 1. Introduction

Today the regulatory authorities require that new drugs have been tested with respect to each enantiomer already at the initial stage of drug development [1,2]. This requires rapid methods for purification of mg-g amounts of the individual enantiomers of the chiral drugs. Such a method is preparative chiral chromatography, performed with a battery of stationary phases with selectivity for different types of compounds and with high chiral capacities. Non-chromatographic methods, such as crystallisation using diastomeric salt formation or asymmetric synthesis, are too time-consuming and tedious for this short-term purpose [3,4].

The trend in preparative chiral chromatography is toward continuous operational modes, such as recycling and simulated moving bed (SMB) [5]. These complex methods are

difficult to optimise properly without computer simulations. The simulation programs, in turn, require the adsorption isotherm parameters for the actual system as input parameters.

These adsorption isotherm parameters can also provide important fundamental mechanistic information about the adsorption behaviour of the phase system. In an earlier study, the theory of non-linear chromatography was used to characterize the chromatographic separation of the enantiomers of some  $\beta$ -blockers using immobilized cellobiohydrolase as stationary phase [6]. It was found that this adsorption was heterogeneous; the enantiomers were adsorbed on one low density site with a strong energy of interaction and on one high density site with weak interaction energy. The high-density sites were denoted type-I sites and were non-chiral. These sites contribute only to the retention of the enantiomers, not to their resolution. The term for the type-I sites is a lumped term describing all types of non-selective interactions, of varying interaction strength and density. However, it should be mentioned that weak low-density adsorption sites

\* Corresponding author. Tel.: +46 18 471 4879;

fax: +46 18 55 5016; mobile: +46 70 425 06 83.

E-mail address: [Torgny.Fornstedt@ytbioteknik.uu.se](mailto:Torgny.Fornstedt@ytbioteknik.uu.se) (T. Fornstedt).

are both difficult to recognise by the chromatographic experiments and less important by the simple reason they do not affect the total retention much. On the other hand, the type-II sites are strong sites which are also enantioselective, so called “true” chiral sites. These sites contribute both to retention and resolution of the enantiomers.

A chiral stationary phase (CSP) consists of an achiral matrix, e.g., porous silica, with chemically or dynamically bonded chiral ligands. These ligands can be small substances, such as Pirkle phases [7] or somewhat larger, such as cyclodextrins [8]. The chiral ligands can also be macromolecules, such as cellulose derivatives [9], macrocyclic glycopeptides [10] or immobilized proteins [6,11]. Most nonlinear adsorption studies made on CSPs so far, has been made on protein phases. The studies showed that the “true” chiral saturation capacity is very low for protein CSPs. Thus, when the sample size is increased the chiral resolution rapidly vanishes [6,11]. Therefore, protein CSPs should be avoided for preparative applications. Instead, CSPs with large chiral capacities should be preferred, such as Chirobiotic T (macrocyclic glycopeptides) and Chiralcel OJ (cellulose), which have been used for preparative applications [9,12]. Kromasil CHI-TBB is a new promising chiral stationary phase consisting of a network polymer that incorporates a bifunctional C<sub>2</sub>-symmetric chiral selector [13,14]. This CSP is aimed at preparative chiral separations of acidic racemates.

The loading capacity of a CSP is a very important parameter. Still, there is a lack of quantitative comparisons made between different CSPs regarding their chiral capacities. The few comparisons made are based on empirical data regarding sample mass purified using different CSPs under various operation conditions and column dimensions [15]. By instead comparing the “true” chiral saturation capacities of different CSPs, a more relevant comparison is possible. Although a large number of nonlinear adsorption studies have been done on protein CSPs, relatively few such studies have been done on high-capacity CSPs designed for preparative purposes. One example of the latter is, a study made by Charton et al. [16] on the adsorption of the enantiomers of methyl mandelate on an immobilized cellulose (Chiralcel OJ) stationary phase. The bi-Langmuir equation best described the adsorption isotherms of these solutes and the monolayer capacity of the chiral type-II sites was approximately 12 times higher than those found for the same chiral compound on the protein column CHIRAL-AGP [11].

The aim of the present study was three-fold:

- to investigate the adsorption behaviour of 2-phenylbutyric acid on Kromasil CHI-TBB using the theory of non-linear chromatography;
- to validate the adsorption isotherm parameters with statistical evaluation methods and to compare the simulated elution profiles with experimental ones using a new function for calculation of the degree of overlap;
- to compare the derived “true” chiral monolayer capacities with those reported for other modern CSPs.

## 2. Theory

### 2.1. Adsorption models

The experimental adsorption data were fitted both to the Langmuir and the bi-Langmuir isotherm models. The Langmuir model accounts well for the adsorption of single components on homogenous surfaces at low to moderate concentrations [17]:

$$q = \frac{aC}{1 + bC} = \frac{bq_s C}{1 + bC} \quad (1)$$

where  $q$  is the stationary phase concentration at equilibrium with the mobile phase concentration  $C$ ; parameter  $a$ , the equilibrium or Henry constant at infinite dilution and  $a$  is also equal to the initial slope of the adsorption isotherm; parameter  $b$ , the equilibrium constant per unit of surface area and  $b$  is therefore related to the adsorption energy. The monolayer capacity or specific saturation capacity of the stationary phase is  $q_s = a/b$ .

In many cases, the surface of the adsorbent used for chromatographic separations is not homogenous. The simplest model for a nonhomogeneous surface is a surface covered with two different kinds of sites which behave independently. Since there are two different adsorption sites on the adsorbent surface in most columns for chiral separation the Langmuir equation must be extended to an equation called the bi-Langmuir isotherm:

$$q = \frac{a_I C}{1 + b_I C} + \frac{a_{II} C}{1 + b_{II} C} = \frac{b_I q_{s,I} C}{1 + b_I C} + \frac{b_{II} q_{s,II} C}{1 + b_{II} C} \quad (2)$$

where  $b_{II}$  usually is much larger than  $b_I$  and  $q_{s,II}$  is much smaller than  $q_{s,I}$ .

### 2.2. Retention factors

The classical retention factor is related to the numerical coefficients of the Langmuir isotherm by the following equation under linear conditions, i.e., at infinite dilution:

$$k = F \frac{\partial q}{\partial C} = Fa \quad (3)$$

where  $F$  is the phase ratio ( $V_s/V_m$ ) and  $k$ , the retention factor. If the stationary phase has a heterogeneous surface with two types of adsorption sites the retention factor is the sum of two contributions originating from type-I and type-II sites. A general expression of the retention factors of the two enantiomers under linear conditions can be expressed as:

$$k = k_I + k_{II} = F(a_I + a_{II}). \quad (4)$$

### 2.3. Calculating band profiles

The equilibrium-dispersive (ED) model [17] was used to calculate the overloaded band profiles. This model assumes constant equilibrium between the stationary and the mobile

phase. The model uses an apparent dispersion term,  $D_a$ , to account for the band-broadening effects due to axial diffusion and assumes instantaneous equilibrium between the stationary and the mobile phase.

$$D_a = \frac{\mu L}{2N} \quad (5)$$

where  $\mu$  is the mobile phase velocity;  $L$ , the column length and  $N$ , the number of theoretical plates. This model is valid when the band profile is more influenced by the nonlinear behaviour of the equilibrium isotherm than by kinetic effects [17]. In the ED model, the mass balance equation for a single component is expressed as follows:

$$u \frac{\partial C}{\partial z} + \frac{\partial C}{\partial t} + F \frac{\partial q}{\partial t} - D_a \frac{\partial^2 C}{\partial z^2} = 0 \quad (6)$$

where  $t$  is the time and  $z$ , the axial position in the column;  $q$ , the concentration of the solute in the stationary phase in equilibrium with  $C$ , the mobile phase concentration of the solute;  $u$ , the mobile phase velocity [17].

In order to get a unique solution to the system of partial differential equations that the mass balance equations constitute it is necessary to complete them by a set of initial and boundary conditions [17]. The initial condition describes the state of the column when the experiment begins, i.e., at  $t=0$ . In this case, the initial conditions correspond to a column empty of sample and containing only mobile and stationary phases in equilibrium:

$$C(t=0, z) = 0 \quad \text{where } 0 \leq z \leq L \quad (7)$$

The boundary condition characterizes the injection. If dispersion effects are neglected it can be regarded as a rectangular pulse with duration  $t_p$  at the column inlet. If the concentration of the injected compound is  $C_0$  we have:

$$C(t, z=0) = C_0 \quad \text{when } 0 \leq t \leq t_p, \quad (8a)$$

$$C(t, z=0) = 0 \quad \text{when } t > t_p \quad (8b)$$

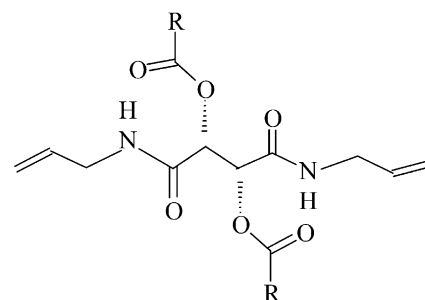
The systems of mass balance equations with the proper isotherm equations should be integrated numerically to obtain the concentration profiles at the column outlet.

### 3. Experimental

#### 3.1. Apparatus

The chromatographic system used consisted of two Jasco PU-1580 intelligent HPLC pumps (Tokyo, Japan). The pump outlets were connected via a low dead-volume PEEK T-connector. All connections were short sections of 0.13 mm PEEK capillaries. The injector was a Jasco AS-1550 Intelligent sampler with a 50  $\mu$ L loop. The detector was an HPLC-spectrophotometer Lamda 1010 from Bischoff (Leonberg, Germany). The refractive index (RI) detector was a Beckman

O,O'-diaroyl-N,N'-diallyl-L-tartaridamide monomer unit



R = 4-t-Bu-C<sub>6</sub>H<sub>4</sub> in Kromasil KR 100-10 CHI-TBB

Fig. 1. The molecular structure of the monomer unit which comprises the network-polymeric stationary phase in Kromasil KR 100-10 CHI-TBB.

156 refractive index detector (Knauer, Berlin 37). The separations were carried out on a Kromasil CHI-TBB column (100 mm  $\times$  4.6 mm I.D., Eka Chemicals AB, Bohus, Sweden). The Kromasil CHI-TBB column consist of a network polymer with incorporating bifunctional C<sub>2</sub>-symmetric chiral selector [13,14], the monomer; O,O'-diaroyl-N,N'-diallyl-L-tartaridamide (see structure in Fig. 1), the polymer is covalent bonded to functionalized silica. The chiral selector is anchored to the network polymer by a crosslinking reaction, which also causes the covalent bonding to the functionalized silica [13]. The column was temperature controlled in a circulating water-bath Model B Lauda (Köningshofen, Germany) at 20.0 °C. A computer data acquisition system using the software CSW version 1.7 DLL was used to record the chromatograms.

#### 3.2. Chemicals

(R)-(-)-2-phenylbutyric acid and (S)-(+)-2-phenylbutyric acid were 99% pure chemicals from Aldrich Chem. Co. (Stockholm, Sweden). The organic solvents used for chromatography were *n*-hexane, 2-propanol, ethyl acetate and methyl *tert*-butyl ether (MTBE); all were of Lichrosolv grade from Merck KGaA (Darmstadt, Germany). Formic acid and acetic acid were of pro analysis grade from Merck KGaA (Darmstadt, Germany).

#### 3.3. Procedures

Staircase frontal analysis was used to acquire adsorption data for the enantiomers of 2-phenylbutyric acid. One pump (A) was connected to a reservoir containing the pure mobile phase, the other (B) to a reservoir containing the enantiomer dissolved in the mobile phase. Using the high-pressure gradient mode of the instrument, a solution of constant B/A concentration was pumped through the column. This concentration was increased stepwise (10 steps) at constant time-intervals for each bulk concentration, resulting

in a staircase chromatogram. Four different bulk concentrations of each enantiomer were used successively as solvent B, which allowed the collection of adsorption data over a broad concentration range. More particularly, 40 data points were acquired for each enantiomer over a concentration range between 7.6  $\mu\text{M}$  and 305 mM, an approximately 40,000-fold range. The flow rate was 0.80 ml/min. The wavelength of the UV-detector was set at 240 or 280 nm. The absorbance data from the detector was transformed into concentration units using a calibration curve derived from absorbance measurements made on the concentration plateaus of the frontal analysis staircase.

Two different dead volumes must be determined using the FA method: the column hold-up volume  $V_0$  and the total dead volume for the staircase experiment  $V_T$ . The latter volume is the entire volume after the T-connector (including  $V_0$ ) and until the column exit. The column hold-up volume,  $V_0$ , was determined to 1.21 mL by injecting the sample and measuring the first-eluted front disturbance. The total dead volume ( $V_T$ ) was determined to be 1.53 mL ( $V_0$  is included in  $V_T$ ) by equilibrating the system with mobile phase from one pump and at a time  $t$  introducing a steep gradient of a mobile phase with a slightly different composition from a second pump. The phase ratio ( $F$ ) was calculated to be 0.376.

The values of the parameters of the Langmuir and bi-Langmuir isotherm expressions (Eqs. (1) and (2)) were calculated using a nonlinear regression method, the Gauss–Newton algorithm with the Levenberg modification, as implemented in the software PCNONLIN 4.2 from Scientic Consulting (Apex, NC, USA). When performing the regression on PCNONLIN, the experimental data were fitted to both the Langmuir and the bi-Langmuir equation. For the bi-Langmuir case, both free and locked parameters were estimated. Locked parameters mean that the software is forced to give one of the sites the same parameters for both enantiomers. Free parameters mean that the software is free to estimate any values for the parameters that fit the experimental data best. Both free and locked bi-Langmuir parameters are presented in Table 1.

Fractions from overloaded eluent chromatograms were taken at 6-s intervals and each fraction was diluted and re-

injected. Using the chromatograms from the re-injections, the molar fraction of each enantiomer was calculated from the peak areas and then the UV-records from the overloaded eluent chromatograms were used to translate the contents of these fractions to enantiomer concentrations.

#### 4. Results and discussions

Kromasil CHI-TBB has been suggested to be well suited for preparative separations of acidic racemates [13,14]. For this CSP, formic or acetic acid is usually recommended as additive to the mobile phase in order to improve the peak shape and the resolution [14,18]. At first, a mobile phase recommended in the literature namely hexane/ethylacetate/formic acid 85/15/0.1, was used. However, the presence of the additive formic acid resulted in a system peak effect with strong peak deformations of the 2-phenylbutyric acid enantiomers. This is illustrated in Fig. 2a showing the chromatogram resulting after the injection of 50  $\mu\text{L}$  of 63.6 mM racemic mixture of the enantiomers (i.e., 31.8 of each enantiomer). The first eluted (S)-enantiomer showed peak tailing with a deformed rear portion and the second eluted (R)-enantiomer showed fronting. We suspected peak deformations due to a co-eluting system peak and made therefore injections of eluent lacking formic acid and recorded the column outlet with a refractive index detector. The RI-chromatogram revealed a system peak eluted between the two enantiomers at a retention time around 5 min (see Fig. 2b). The fronting deformation caused by a system peak has been described previously both theoretically [19] and experimentally [20]. Fig. 3 shows the chromatogram resulting after injection of a sample with a 10-fold higher concentration (320 mM) of only the later-eluted (R)-enantiomer using the same eluent. Here, the fronting deformation has developed to an almost rectangular zone with a valley at its top.

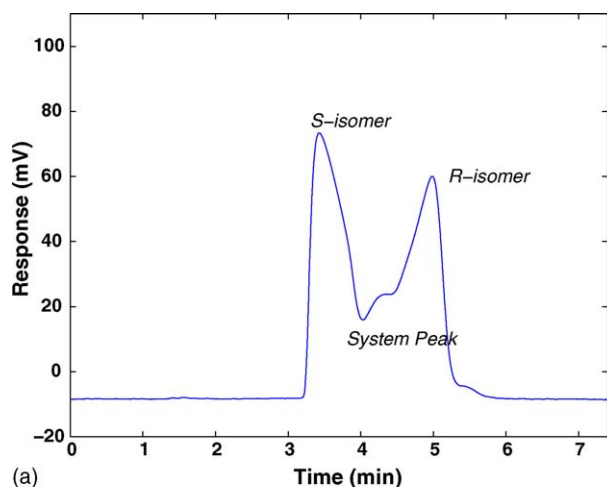
The system peak probably originated from the presence of formic acid in the eluent. When acetic acid was tested as an alternative additive, the enantiomer peaks of 2-phenylbutyric acid were still disturbed. In addition, acetic acid did not reduce the peak tailing and improve the peak resolution as efficient as the stronger formic acid did.

##### 4.1. Choice of mobile phase modifier

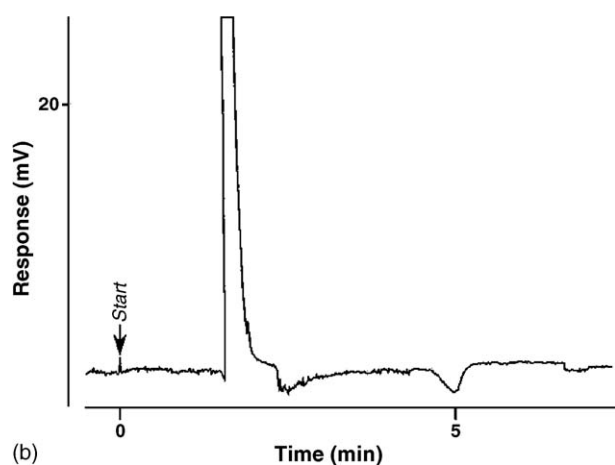
The deformation effects made it impossible to acquire isotherms of 2-phenylbutyric acid through frontal analysis (FA) and did also deteriorate the preparative separation at larger sample loads. Since similar deformation effects of the solute bands occurred for both of the acidic additives it was concluded that an optimal modifier would be one which did not require an additive. Mobile phases were tested composed of *n*-hexane and one of the three different modifiers ethylacetate, 2-propanol or methyl *tert*-butyl ether (MTBE). With ethylacetate or 2-propanol as modifiers the peak tailing was too strong and the resolution was bad, even at high modifier

Table 1  
Free and locked bi-Langmuir isotherm parameters for (R)- and (S)-2-phenylbutyric acid. The relative standard deviations of the parameter estimates are in parenthesis

Type of site	$a$	$b$ (mM <sup>-1</sup> )	$q_s$ (mM)
Free parameters			
R, I	6.53 (5.4)	0.01368 (4.7)	477.3
S, I	4.36 (4.9)	0.00994 (4.5)	438.6
R, II	19.86 (1.7)	0.15185 (5.3)	130.8
S, II	14.39 (1.4)	0.11673 (4.6)	123.3
Locked parameters			
R, I	5.10 (4.4)	0.01130 (3.9)	451.3
S, I	5.10 (4.4)	0.01130 (3.9)	451.3
R, II	20.27 (1.3)	0.12022 (3.2)	168.6
S, II	14.18 (1.7)	0.13971 (5.4)	101.5



(a)



(b)

Fig. 2. (a) The chromatogram shows peak deformations caused by a system peak after the injection of 50  $\mu\text{L}$  of a 63.6 mM racemate of 2-phenylbutyric acid. The mobile phase was *n*-hexane/ethyl acetate (85/15) with 0.1% formic acid. For other conditions, see Section 3. (b) The chromatogram shows a refractive-index trace after the injection of 50  $\mu\text{L}$  of eluent lacking the acid, i.e. *n*-hexane/ethyl acetate (85/15) using the same mobile phase as in (a). A refractive index (RI) detector was used to register the eluate. Otherwise the same conditions as in (a).

contents. When MTBE was used as modifier the peak tailing was less pronounced as compared to the use of the other two modifiers and the resolution between the peaks was good. The best composition of this mobile phase was a 90/10 mixture of *n*-hexane/MTBE, resulting in peaks with moderate retention times, low peak tailing and good resolution.

#### 4.2. Determination of adsorption isotherm parameters and validation of their models

The adsorption isotherms were measured by frontal analysis and the adsorption isotherm parameters were validated in two ways: (1) rival isotherm models were compared using statistical calculations (*F*-test) and (2) simulated elution profiles, using the best isotherm parameters, were compared with experimental ones using an overlap function.

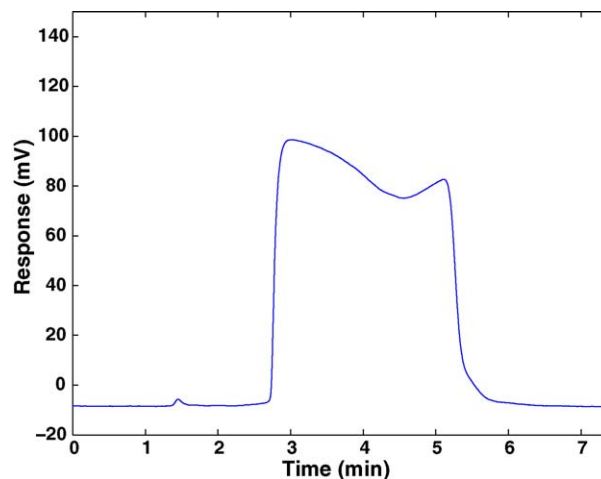


Fig. 3. The chromatogram shows a strong peak deformation caused by a large system peak after the injection of 50  $\mu\text{L}$  320 mM of (R)-2-phenylbutyric acid. Otherwise the same conditions as in Fig. 2a.

#### 4.2.1. Determination of adsorption isotherm parameters

The single component isotherms of the two compounds were measured by using the FA method in the staircase mode (see Section 3). The adsorption data were fitted to both the Langmuir and the bi-Langmuir (free and locked) equations and both sets of parameters are presented in Table 1. The numerical values of the free and locked parameters are of similar sizes. The locked *a* and *b* terms for the type-I site are identical for both enantiomers. Thus, this site, which is the one with the highest saturation capacity ( $q_s = a/b = 451$  mM), is probably nonchiral. The type-II site, which is responsible for the chiral recognition, has an unusually large saturation capacity  $q_s = a/b = 101.5$  mM for the (S)-enantiomer and 168.6 mM for the (R)-enantiomer (cf. locked parameters in Table 1).

#### 4.2.2. Validation of the adsorption isotherm model and its parameters

Successful completion of the regression required weighting of the data points. The weight is equal to  $1/q_{\text{pred}}$ , where  $q_{\text{pred}}$  is the stationary phase concentration predicted by the model. This assumes that the relative error is constant. The free bi-Langmuir model fitted the experimental data much better than the Langmuir model. This was obvious from a visual comparison and was also concluded by comparison of the values of the residuals used in an *F*-test [21] on the models. For both enantiomers the *F*-test was larger than 926 upon comparing the results of the free bi-Langmuir model to those of the Langmuir model. The critical value of *F* ( $P = 0.05$ ,  $\text{d.f.}_2 = 36$ ,  $\Delta\text{d.f.} = 2$ ) is 3.3; where *P*,  $\text{d.f.}_2$  and  $\Delta\text{d.f.}$  are the level of significance, degrees of freedom for the bi-Langmuir model and the difference in degrees of freedom between the models, respectively. If the calculated value is larger than the critical value there is significant difference between the two models, so in this case the bi-



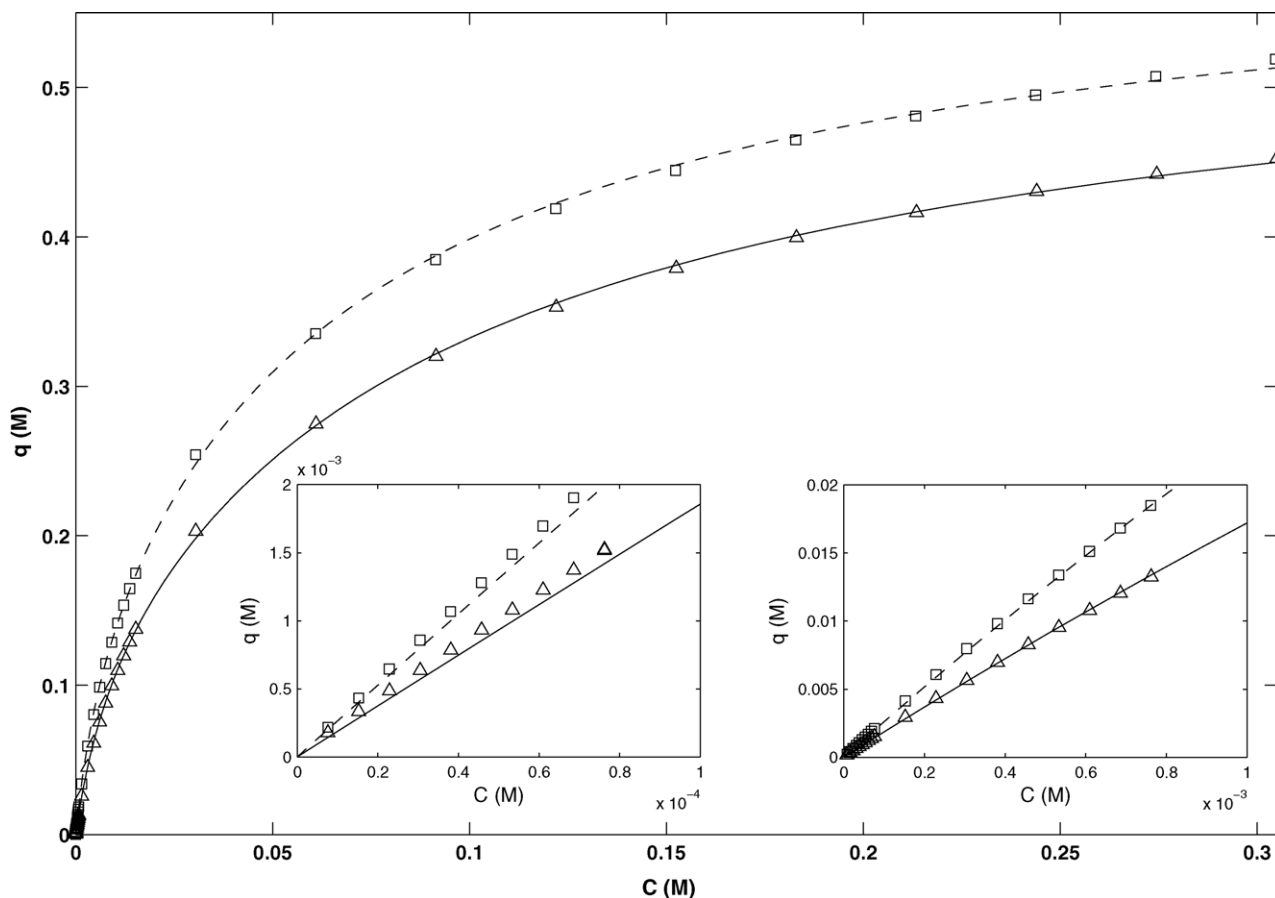


Fig. 4. Experimental and calculated adsorption isotherms for (R) and (S)-2-phenylbutyric acid. The symbols are experimental data; (S)-enantiomer ( $\Delta$ ), (R)-enantiomer ( $\square$ ) and the lines are calculated using the free bi-Langmuir isotherm parameters from Table 1: (S)-enantiomer (solid), (R)-enantiomer (dashed). The main figure shows the high concentration range (below 305 mM). The left inset shows the low-concentration range (below 0.1 mM) and the right inset the medium-concentration range (below 1.0 mM), respectively. The mobile phase was *n*-hexane/MTBE (90/10). For other experimental conditions: see Section 3.

Langmuir equation fits the data significantly better than the Langmuir equation. This statistical result confirms the validity of our assumption of a two-site surface. When comparing the results of the free bi-Langmuir model to those of the locked bi-Langmuir model, both seem to fit the experimental data well upon visual comparison, but the *F*-test was larger than 17.0 and the critical value of *F* ( $P=0.05$ ,  $d.f._2=72$ ,  $\Delta d.f.=2$ ) is 3.1. This statistical result shows that the free bi-Langmuir parameters fits the experimental data significantly better than the locked ones, but the difference is much smaller as compared to when comparing one and two-site models.

Fig. 4 shows the experimental adsorption data (symbols) acquired by the FA method. The lines are the isotherm functions calculated using the free bi-Langmuir adsorption isotherm parameters (cf. Table 1). The calculated isotherms are in excellent agreement with the experimental ones. In Fig. 4, the isotherms are linear both in the low, 0–0.1 mM (cf. Fig. 4: left inset), and in the intermediate concentration ranges, 0–1 mM (cf. Fig. 4: right inset). But, at the high concentration range, 0–300 mM (cf. Fig. 4: main) the isotherms are strongly nonlinear.

#### 4.3. Validation of simulated elution profiles

The validation of an isotherm model and its parameters requires comparison between calculated overloaded band profiles and experimental profiles recorded under the same conditions. In order to quantify how well the simulation fits the experimental data we defined the *overlap* to be,

$$\frac{\int_0^{\infty} \min[c_{\text{sim}}(t), c_{\text{exp}}(t)] dt}{\int_0^{\infty} c_{\text{sim}}(t) dt}, \quad (9)$$

where  $c_{\text{exp}}(t)$ ,  $c_{\text{sim}}(t)$  is the experimental and simulated response at time  $t$ . This equation measures the relative amount of the peak-area that differs when comparing the simulated and measured elution profiles. When the experimental and simulated elution profiles coincide perfectly the overlap is 100% and when they are totally separated the overlap is 0. In this study, both single and binary elution profiles were used to validate the adsorption isotherm parameters.

##### 4.3.1. Single-component band profiles

The experimental single-component band profiles of both enantiomers were compared with the calculated ones using

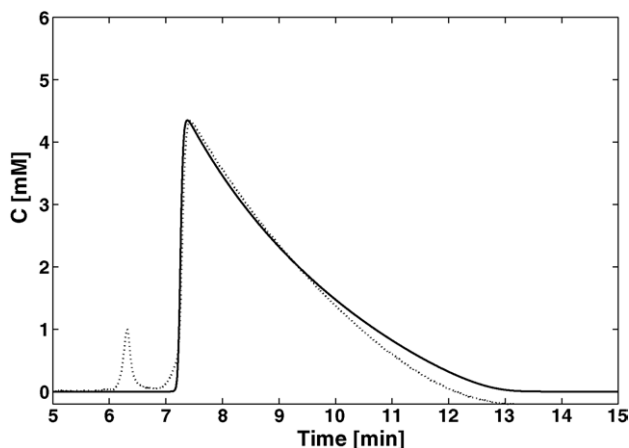


Fig. 5. Comparison between experimental (dotted line) and calculated (dashed line) overloaded elution band profiles resulting from the injection of 25  $\mu$ L 305.0 mM of (S)-2-phenylbutyric acid. The line is calculated using the free bi-Langmuir adsorption isotherm parameters from Table 1. Other experimental conditions as in Fig. 3.

both the free and the locked bi-Langmuir parameters. The (S)-enantiomer in Fig. 5 and the (R)-enantiomer in Fig. 6 show the comparison of the experimental (dotted line) and calculated overloaded single-elution profiles (dashed line) for the two enantiomers using the free bi-Langmuir parameters. The calculated elution profiles (free bi-Langmuir parameters, cf. Table 1) agreed very well with the experimental profiles in both cases and the overlaps are quite good, 88.7% for the (S)-enantiomer and 92.0% for the (R)-enantiomer. The overlap for the (S)-enantiomer is calculated only between 6.5 min and 13.0 min because the contamination peak eluting before the (S)-enantiomer lowered the overlap to 74.2%. The locked bi-Langmuir parameters (cf. Table 1) also gave high overlaps, 87.0% for the (S)-enantiomer and 91.0% for the

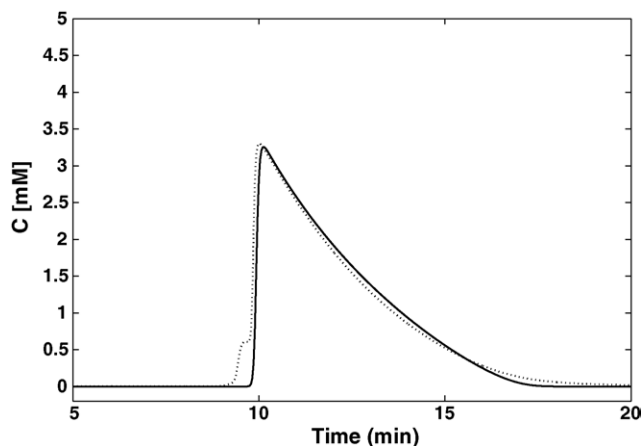


Fig. 6. Comparison between experimental (dotted line) and calculated (solid line) overloaded elution band profiles (dotted line) resulting from the injection of 25  $\mu$ L 304.7 mM of (R)-2-phenylbutyric acid. The line is calculated using the free bi-Langmuir adsorption isotherm parameters from Table 1. Other experimental conditions as in Fig. 3.

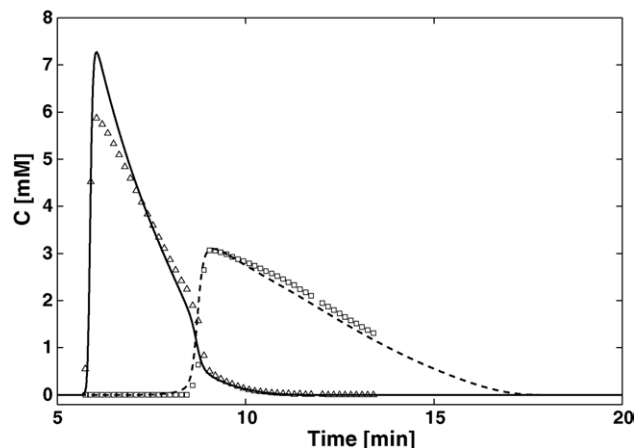


Fig. 7. Comparison between experimental and calculated binary band profiles resulting from the injection of 50  $\mu$ L 400.0 mM racemate of 2-phenylbutyric acid. Symbols denote experimental data: (S)-enantiomer ( $\Delta$ ), (R)-enantiomer ( $\square$ ). Lines are calculated data using the free bi-Langmuir adsorption isotherm parameters from Table 1: (S)-enantiomer (solid), (R)-enantiomer (dashed). Other experimental conditions as in Fig. 3.

(R)-enantiomer, but not as high as the overlaps for the free parameters.

#### 4.3.2. Binary-component band profiles

In binary mixtures, the individual band profiles were determined in the mixed regions by analysis of collected fractions. A comparison was made between experimental (symbols) and theoretical profiles (lines) for 1:1 (Fig. 7) and 1:3 (Fig. 8) mixtures of the (S)-enantiomer and the (R)-enantiomer. Fig. 7 shows the injection of such a high amount as 50  $\mu$ L 400 mM racemic mixture of 2-phenylbutyric acid (i.e., 200 mM of each enantiomer). Fig. 8 shows the overloaded injection of 50  $\mu$ L of 285 mM of the (R)-enantiomer and 95 mM of the

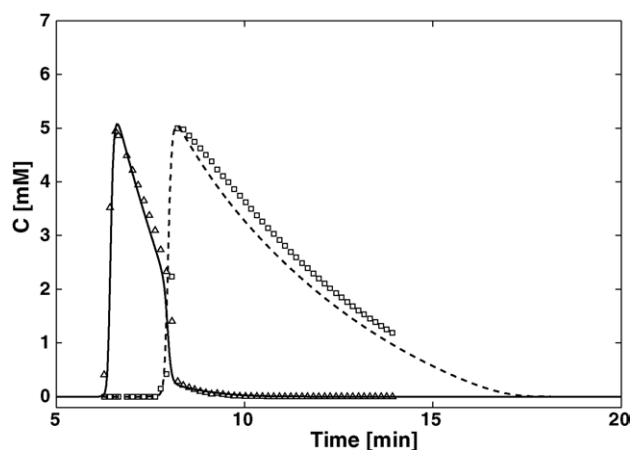


Fig. 8. Comparison between experimental and calculated binary band profiles after the injection of 50  $\mu$ L 97.0 mM (S)-2-phenylbutyric acid and 287.0 mM (R)-2-phenylbutyric acid (a 1/3 mixture). Symbols denote experimental data: (S)-enantiomer ( $\Delta$ ), (R)-enantiomer ( $\square$ ). Lines are calculated data using the free bi-Langmuir adsorption isotherm parameters from Table 1: (S)-enantiomer (solid), (R)-enantiomer (dashed). Other experimental conditions as in Fig. 3.

(S)-enantiomer, 3/1 mixture. The agreement between the experimental profiles and those calculated using the free bi-Langmuir parameters was good. The most significant deviation was the height of the first peak in Fig. 7. The overlap in the elution profiles for the injections was 95.8% in Fig. 7 and 94.9% in Fig. 8 using the free bi-Langmuir parameters. If the locked bi-Langmuir parameters were used the overlaps were only 76.0% and 81.7% for Figs. 7 and 8, respectively.

#### 4.4. Identification of the adsorption sites on Kromasil CHI-TBB

The validation of the elution profiles (see above) confirms that the adsorption is heterogeneous and that its best descriptors were the free bi-Langmuir parameters. It is difficult to judge which site is chiral from only the free parameters. However, the locked parameters were almost as good and this indicates that the high-capacity site is nonchiral.

A confirmation of the identification of the adsorption sites was provided by the overlay of the individual staircase chromatograms of the respective enantiomer (see Fig. 9). At the first to the third steps (at 30.5, 61.0 and 91.5 mM, respectively) the breakthrough fronts of the two enantiomers are separated from each other while at the fourth step (at 122 mM) there is no visible separation of the break-through fronts. The separation factor ( $\alpha$ ) for each step was calculated by first measure the retention factor in the following way. The retention factor of the actual step ( $k_{\text{Step}}$ ) was calculated by measuring its retention time ( $T_{R,\text{Step}}$ ) at the half-height of the step and by subtracting and dividing with the total correction time  $T_T$  (derived from  $V_T$ , see Section 3) according to  $k_{\text{Step}} = T_{R,\text{Step}} - T_T / T_T$ . Then the separation factor was calculated by  $\alpha = k_{\text{Step}} / k_{\text{Step}}$  where the nominator was the retention factor of the more retained enantiomer. The assumption was made that the chiral sites reach saturation at  $\alpha < 1.1$ . The  $\alpha$

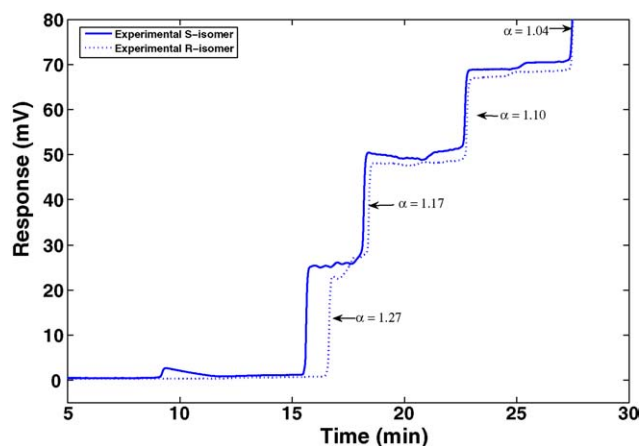


Fig. 9. The first four steps (out of 10) of the overlaid individual staircase chromatogram for (S) and (R)-2-phenylbutyric, respectively. The bulk concentration, of each enantiomer, was 305 mM. Other experimental conditions as in Fig. 3.

values for the first four steps in Fig. 9 were 1.27, 1.17, 1.10 and 1.04, respectively. Thus, the chiral capacity should be somewhere above 100 mM, which is in the same magnitude as the type-II sites in Table 1 (for both free and locked parameters). The saturation capacity of the best type-II values (free parameters) is 131 mM for (R)-(-)-2-phenylbutyric acid and 123 mM for (S)-(+)-2-phenylbutyric. Above the fourth step in Fig. 9, there is no resolution, still both enantiomer fronts are retained. This confirms that the high-capacity site is non-chiral.

#### 4.5. Comparison with other CSPs

It is possible to isolate and determine both strengths and capacities of the chiral sites of any CSP by using theory of non-linear chromatography as a tool. For preparative purposes such a quantitative determination of the saturation capacity of the chiral site is an extremely important piece of information. Even without this quantitative determination, it is indicated that the pure chiral site of the studied column (Kromasil CHI-TBB) has a strikingly large capacity, considering the large amounts of 2-phenylbutyric acid accommodated using an analytical-size column, almost 2 mg of each enantiomer per gram adsorbent, while retaining at least partial peak resolution (cf. Fig. 7).

The “true” chiral capacities for the present system are given in Table 2, in comparison with three systems using protein columns (CHIRAL-AGP and CBH) and with three systems using cellulose-derivative stationary-based phases (Chiralcel OJ and OB). It should be noted that a system represent not only the type of CSP but also the chiral solute and that such a quantitative comparison should be complemented with many different solutes for the various CSPs considered. This is because the chiral capacity is dependent also on the type of solute. It should also be mentioned that the nonlinear regression and choice of adsorption models should, if possible, be done in a standardized way in a systematic comparison. However, the Table 2 provide a good insight of the value of such a study. As can be seen in Table 2, the chiral (type-II site) saturation capacity for the compound methyl mandelate on CHIRAL-AGP is, on the average, 2.15 mM whereas for the compound 2-phenylbutyric acid the value is 3.8 mM. Moreover, Chiralcel OJ has a chiral capacity of 85.3 mM for ketoprofen, whereas it is 25.4 for the compound methyl mandelate (cf. Table 2).

The chiral capacities of the three protein phases in Table 2 are, on the average, 2.3 mM whereas the corresponding averaged coefficient for the three cellulose-derivative systems is 57.2 mM. Thus, the cellulose-derivative-based CSPs has, on the average, a 25-fold times larger chiral capacity than the protein CSPs. By contrast, the averaged saturation capacity of the chiral site of Kromasil CHI-TBB (127 mM) is 1.5 times larger than the largest capacity of any of the cellulose-derivative-based CSPs in Table 2 (ketoprofen on Chiralcel OJ). This result is in contrast to a previous comparison where tartardiamide phases has markedly lower saturation capacity



Table 2  
Saturation capacity for different chiral stationary phases

Reference	Stationary phase (type)	Solute	Isomer	$q_{s,I}$ (mM)	$q_{s,II}$ (mM)
This work	Kromasil CHI-TBB (polymer)	2-Phenylbutyric acid	R	477.3	130.8
			S	438.6	123.3
[11]	CHIRAL-AGP (protein)	2-Phenylbutyric acid (pH 5.0)	R	29.4	3.6
			S	29.4	4.0
[11]	CHIRAL-AGP (protein)	Methyl mandelate (pH 5.0)	S	12.6	2.1
			R	12.6	2.2
[6]	CHIRAL-CBH I (protein)	Propranolol (298.1 K; pH 5.5)	R	23.1	0.9
			S	21.5	0.8
[16]	Chiralcel OJ (cellulose)	Methyl mandelate	D	549	25.4
			L	549	25.4
[22]	Chiracel OJ (cellulose)	Ketoprofen	R	598	85.3
			S	598	85.3
[23]	Chiralcel OB (cellulose)	1-Indanol	R	655	47.0
			S	820	74.5

as compared to polysaccharide-based phases (cf. Fig. 4 in [15]). The reason for the different result can be that the latter comparison was based on empirical data of sample amount purified instead of standardized coefficients but also that an acid was included in the eluent destroying the resolution at high-concentration injections (see above).

The solute 2-phenylbutyric acid used in this study (on CHI-TBB) was also used on the protein column CHIRAL-AGP. A comparison showed that the chiral capacity on Kromasil CHI-TBB was 33 times larger as compared on CHIRAL-AGP. The staircase steps of the two enantiomers of the CHIRAL AGP system had a combined elution at 3 mM or higher when  $\alpha < 1.1$  (unpublished results of system in [11]). This confirmed the accuracy of our approach coefficient-based comparison since 33 times 3 mM is around 100 mM which is the concentration when  $\alpha < 1.1$  for Kromasil CHI-TBB (see above).

The saturation capacities of the nonchiral type-I sites are also presented in Table 2. The averaged value for Kromasil CHI-TBB (458 mM) is comparable to that of the cellulose-derivative-based systems (569 mM) and also to the capacity of common homogenous systems, such as C18 columns, using the simple Langmuir equation. As an example, in a recent study by Forssén et al., the capacities for two steroids adsorbed on a modern C18 column were found to be 475 and 650 mM, respectively [24]. Interestingly, the corresponding averaged value for the protein-based phases in Table 2 is 21.4 mM, a value which is around 25 times smaller than for the chiral phases using less bulky substances as immobilized selectors (cf. Table 2).

## 5. Conclusions

In this study, the adsorption behaviour of the enantiomers of the model compound 2-phenylbutyric acid was investi-

gated on the new chiral stationary phase Kromasil CHI-TBB. The bi-Langmuir equation fitted best to the acquired adsorption isotherms, indicating a heterogeneous surface. This model allowed isolation of the “true” chiral sites as well as quantitative determination of their adsorption strength and capacity. The derived adsorption data were compared with the adsorption data reported earlier for CSPs aimed at both analytical and preparative purposes. The comparison showed that Kromasil CHI-TBB apparently has an unusually large capacity for the chiral sites. Thus, the “true” chiral capacity was found to be 33 times larger than for the protein phase CHIRAL-AGP using the same model compound and 1.5 times larger the largest value found in the literature for any cellulose derivative CSP (Chiralcel OJ separating ketoprofen). However, a prerequisite for the large chiral capacity of Kromasil CHI-TBB is that the recommended acidic additive is lifted out.

We could also demonstrate that in general the number of non-chiral sites are around 25 times fewer on chiral phases based on immobilized proteins as compared to such using less bulky substances as immobilized selectors or of common capacities on C18 systems (cf. Table 2).

We recommend that comparisons of the loading capacities of CSPs should be based on the coefficients for the “true” chiral capacity, obtained by using the theory of nonlinear LC as a tool. This should provide a more relevant and standardized way to compare different CSPs as compared to the previous approach based on data of sample amount purified during various operation conditions and different column dimensions [15]. However, there exist today relatively few nonlinear adsorption studies done on high-capacity CSPs as compared to protein CSPs. A larger number of such data on preparative CSPs with many different solutes is necessary since the “true” chiral capacity is dependent not only on the type of CSP but also on the type of solute.

## Acknowledgments

The author thanks Ph.D. Gustaf Götmar for always being available when help was needed and Ph.D. Patrik Forssén for statistical support and advice concerning overlap functions. The author thanks also AstraZeneca R&D (Möln dal, Sweden) for the column, chemicals and solutions.

## References

- [1] W.H. De Camp, *Chirality* 1 (1989) 2.
- [2] FDA's policy statement for the development of new stereoisomeric drugs, <http://www.fda.gov/cder/guidance/stereo.htm> (june 2004).
- [3] R. Valentine, A.J. Russell, E.J. Beckman, in: *Book of Abstracts, Proceedings of the 211th ACS National Meeting, New Orleans, LA, 24–28 March, 1996, I&EC-145*.
- [4] P.J. Walsh, J. Balsells, T. Davis, J.M. Betancort, *Abstracts of Papers, American Chemical Society, 2001, 221st ORGN-264*.
- [5] R.M. Nicoud, G. Fuchs, P. Adam, M. Bailly, E. Küsters, F.D. Antia, *Chirality* 5 (1993) 267.
- [6] T. Fornstedt, G. Zhong, Z. Benseniti, G. Guiochon, *Anal. Chem.* 68 (1996) 2370.
- [7] W.H. Pirkle, J.M. Finn, *J. Org. Chem.* 46 (1986) 2935.
- [8] D.W. Armstrong, J. Zukowski, *J. Chromatogr. A* 666 (1994) 445.
- [9] Y. Okamoto, Y. Kaida, *J. Chromatogr. A* 666 (1994) 403.
- [10] D.W. Armstrong, Y. Tang, S. Chen, Y. Zhou, C. Bagwell, J.-R. Chen, *Anal. Chem.* 66 (1994) 1473.
- [11] G. Götmar, N.R. Albareda, T. Fornstedt, *Anal. Chem.* 74 (2002) 2950.
- [12] L. Thunberg, S. Adersson, S. Allenmark, J. Vessman, *J. Pharm. Biomed. Anal.* 27 (2002) 431.
- [13] S.G. Allenmark, S. Andersson, P. Möller, D. Sanchez, *Chirality* 7 (1995) 248.
- [14] S. Andersson, S. Allenmark, P. Möller, B. Persson, D. Sanchez, *J. Chromatogr. A* 741 (1996) 23.
- [15] E. Francotte, *J. Chromatogr. A* 906 (2001) 379.
- [16] F. Charton, S. Jacobson, G. Guiochon, *J. Chromatogr.* 630 (1993) 21.
- [17] G. Guiochon, S. Golshan-Shirazi, A.M. Katti, *Fundamentals of Preparative and Nonlinear Chromatography*, Academic Press, Boston, MA, 1994.
- [18] A.C. Löwendahl, S.G. Allenmark, *Chirality* 9 (1997) 167.
- [19] T. Fornstedt, G. Guiochon, *Anal. Chem.* 66 (1994) 2116.
- [20] T. Fornstedt, G. Guiochon, *Anal. Chem.* 66 (1994) 2686.
- [21] J. Gabrielsson, D. Weiner, *Pharmacokinetic and Pharmacodynamic Analysis: Concepts and Applications*, second ed., Swedish Pharmaceutical Society, Swedish Pharmaceutical Press, Stockholm, Sweden, 1997.
- [22] F. Charton, M. Bailly, G. Guiochon, *J. Chromatogr. A* 687 (1994) 13.
- [23] D. Zhou, K. Kaczmarek, A. Cavazzini, X. Liu, G. Guiochon, *J. Chromatogr. A* 1020 (2003).
- [24] P. Forssén, J. Lindholm, T. Fornstedt, *J. Chromatogr. A* 991 (2003) 31.